CHEST RADIOLOGY

Clinical implications of microvascular CT scan signs in COVID-19 patients requiring invasive mechanical ventilation

Giorgia Dalpiaz[1] · Lorenzo Gamberini[2] · Aldo Carnevale[3] · Savino Spadaro[4] · Carlo Alberto Mazzoli[2] ·
Sara Piciucchi[5] · Davide Allegri[6] · Chiara Capozzi[7] · Ersenad Neziri[8] · Maurizio Bartolucci[9] · Francesco Muratore[10] ·
Francesca Coppola[11] · Antonio Poerio[12] · Emanuela Giampalma[13] · Luca Baldini[14] · Tommaso Tonetti[15] ·
Iacopo Cappellini[16] · Davide Colombo[17,18] · Gianluca Zani[19] · Lorenzo Mellini[20] · Vanni Agnoletti[21] ·
Federica Damiani[22] · Giovanni Gordini[2] · Cristiana Laici[23] · Giuliano Gola[24] · Antonella Potalivo[25] ·
Jonathan Montomoli[26] · Vito Marco Ranieri[15] · Emanuele Russo[21] · Stefania Taddei[27] · Carlo Alberto Volta[4] ·
Gaetano Scaramuzzo[4]

Abstract

Purpose COVID-19-related acute respiratory distress syndrome (ARDS) is characterized by the presence of signs of microvascular involvement at the CT scan, such as the vascular tree in bud (TIB) and the vascular enlargement pattern (VEP). Recent evidence suggests that TIB could be associated with an increased duration of invasive mechanical ventilation (IMV) and intensive care unit (ICU) stay. The primary objective of this study was to evaluate whether microvascular involvement signs could have a prognostic significance concerning liberation from IMV.

Material and methods All the COVID-19 patients requiring IMV admitted to 16 Italian ICUs and having a lung CT scan recorded within 3 days from intubation were enrolled in this secondary analysis. Radiologic, clinical and biochemical data were collected.

Results A total of 139 patients affected by COVID-19 related ARDS were enrolled. After grouping based on TIB or VEP detection, we found no differences in terms of duration of IMV and mortality. Extension of VEP and TIB was significantly correlated with ground-glass opacities (GGOs) and crazy paving pattern extension. A parenchymal extent over 50% of GGO and crazy paving pattern was more frequently observed among non-survivors, while a VEP and TIB extent involving 3 or more lobes was significantly more frequent in non-responders to prone positioning.

Conclusions The presence of early CT scan signs of microvascular involvement in COVID-19 patients does not appear to be associated with differences in duration of IMV and mortality. However, patients with a high extension of VEP and TIB may have a reduced oxygenation response to prone positioning.

Trial Registration: NCT04411459

Keywords Novel coronavirus disease 2019 · Acute respiratory distress syndrome · Pulmonary perfusion · Thoracic imaging · Mechanical ventilation

Abbreviations

ARDS	Acute respiratory distress syndrome
ICU	Intensive care unit
CT	Computed tomography
VEP	Vascular enlargement pattern
TIB	Tree in bud
GGOs	Ground-glass opacities
NIV	Non-invasive ventilation
IMV	Invasive mechanical ventilation
VFD	Ventilator-free days
SAPS II	Simplified acute physiology score
SOFA	Sequential organ failure assessment
LDH	Lactate dehydrogenase
CRP	C-reactive protein
PP	Prone positioning
IQR	Interquartile range

✉ Lorenzo Gamberini
 lorenzo.gamberini86@gmail.com

Extended author information available on the last page of the article

Introduction

COVID-19 is a multisystem syndrome due to cellular infection via the ACE 2 receptors by SARS-CoV-2. This syndrome most commonly involves the respiratory system, with 15% of cases showing severe respiratory failure and 5% requiring intensive care unit (ICU) admission for acute respiratory distress syndrome (ARDS) or multiorgan failure [1].

Thrombotic complications are frequently observed in COVID-19 patients [2] and, especially for COVID-19 related ARDS, the observed incidence of pulmonary embolism (PE) and alveolar-capillary microthrombosis are significantly higher than for other ARDS causes [3, 4].

A combination of conventional mechanisms of clot formation and immunothrombosis (particularly for smaller clots) seems to underlie these manifestations, and more recent insights about the interactions between SARS-CoV-2 and the vascular endothelium led to the definition of a COVID-19-associated coagulopathy.

This syndrome is characterized by mild thrombocytopenia, mildly prolonged prothrombin time, increased fibrinogen and raised D-dimer, all of which are more pronounced as disease severity increases [5, 6].

From the histopathological point of view, other than the classical signs of ARDS such as diffuse alveolar damage and hyaline membrane formation, some distinctive pulmonary microvascular abnormalities occur in COVID-19, including intravascular fibrin deposition, perivascular monocyte infiltration, angiogenesis and microthrombi formation [4].

Endothelial inflammation and microthrombosis can justify a series of CT scan abnormalities, such as vascular enlargement pattern (VEP) and vascular tree in bud (TIB), which have been increasingly described in COVID-19 CT scans [7, 8].

The VEP is characterized by dilatation of pulmonary vessels around and within the lung abnormalities on CT images [8, 9], and different descriptive approaches for VEP were adopted in the available literature, such as vascular thickening [10], subsegmental vessels greater than 3 mm [11] or dilated small vessels in the lesion [12].

It appears to be related to the vasodilatation and damage characterized by endothelial injury and enhanced permeability due to the massive accumulation of pro-inflammatory factors in the lung [13]. An increased representation of the VEP is observed along with the increase in the extent of ground-glass opacities (GGOs) and with the clinical severity of COVID-19 symptoms [8].

On the other hand, TIB is the expression of pulmonary microthrombosis that enhances the peripheral pulmonary vessels on CT imaging, therefore producing the TIB pattern [14].

Vascular TIB identification was correlated with an increased duration of mechanical ventilation (MV) and length of hospital stay in a cohort of 39 critically ill invasively ventilated COVID-19 patients [7].

It is not clear if these radiological signs represent only an expression of the extension of the COVID-19-related lung inflammation or if they could have an independent role in determining the severity of the clinical manifestations and the duration of invasive mechanical ventilation (IMV). Moreover, no evidence exists that patients responding differently to some of the COVID-19 related ARDS treatments, such as prone positioning, have different patterns of vascular involvement [15].

Therefore, the primary objective of this study was to assess whether the presence of microvascular damage signs (VEP and TIB) in the chest CT scans acquired within 3 days before or after endotracheal intubation could be independently associated with prolonged IMV in critically ill COVID-19 patients.

Secondary objectives were to find eventual influences of the extension of these signs on the response to prone positioning and ICU outcome measures.

Material and methods

Setting and ethics

This is a secondary analysis of patients enrolled in a previous prospective study [16] initially conducted in 15 ICUs from Italian hospitals between February 22 and May 4, 2020. The data from another ICU obtained after the publication of the first paper were included in the present report.

The study was approved by the Institutional Review Board of the study coordinator centre (Maggiore Hospital, Bologna, Italy, approval number: 273/2020/OSS/AUSLBO) and by each institutional review committee of the participating hospitals. Informed consent was partially waived according to the approval of the local Ethics committee and analysis was conducted on anonymized individual data. The study was registered in ClinicalTrials.gov (NCT04411459).

Outcome measures

The primary outcome measure was the number of ventilator-free days (VFDs) at day 28 (see below for the full definition) between two groups based on the presence/absence of vascular TIB [7] or VEP.

Secondary outcome measures were the differences in VFD at day 28, PaO_2/FiO_2 ratio change after pronation and ICU mortality between groups of patients showing different extensions of the microvascular and parenchymal signs. In particular, the microvascular involvement of 3 or more lobes

for VES and TIB and the parenchymal involvement of over 50% for the parenchymal signs were used to define groups of patients with extended radiologic involvement.

Definitions

Vascular TIB was defined as the presence of dilated peripheral subpleural pulmonary small vessels with a branching aspect resembling a budding tree [7, 17].

VEP was defined as an ectasia of segmental and subsegmental vessels with a diameter larger than expected for the point within the vascular tree, characterized by: (a) vessel diameter larger than that in adjacent portions of the non-diseased lung, (b) vessel diameter larger than that in comparable regions of the non-diseased contralateral lung, or (c) focal dilatation or non-tapering of vessels as they course towards the lung periphery [18].

Detailed images of TIB and VEP are available in Fig. 1.

For the other signs, the definitions were referred to the Glossary of Terms for Thoracic Imaging of the Fleischner Society [19].

Mechanical ventilation was considered invasive if delivered through an endotracheal tube or a tracheostomy cannula. The duration of IMV was defined as the time elapsed from intubation to successful extubation or successful permanent disconnection from mechanical ventilation for tracheostomized patients. This latter was considered effective if sustained 24 h per day. VFDs at 28 days were defined as 28 minus the number of days elapsed from the last successful extubation in intubated patients, whether or not NIV was used after extubation. VFDs were defined as zero in patients who died during the 28 days regardless of their extubation status. In tracheostomized patients, intermittent disconnections were not counted and VFD were defined as 28 minus the number of days from the last successful sustained disconnection from mechanical ventilation [20].

Inclusion and exclusion criteria

To be included in the present study, patients should be tested positive for SARS-CoV-2 infection (confirmed by real-time reverse transcription-polymerase chain reaction assays), older than 18 years, undergo IMV, fulfil the criteria for ARDS according to the Berlin definition [21], and have at least one CT scan available performed within three days before or after orotracheal intubation.

The single non-inclusion criterion was the use of non-invasive ventilation (NIV) during the entire clinical course.

Sample size calculation

The sample size was determined considering 5 VFD as a clinically important difference on a baseline mean of
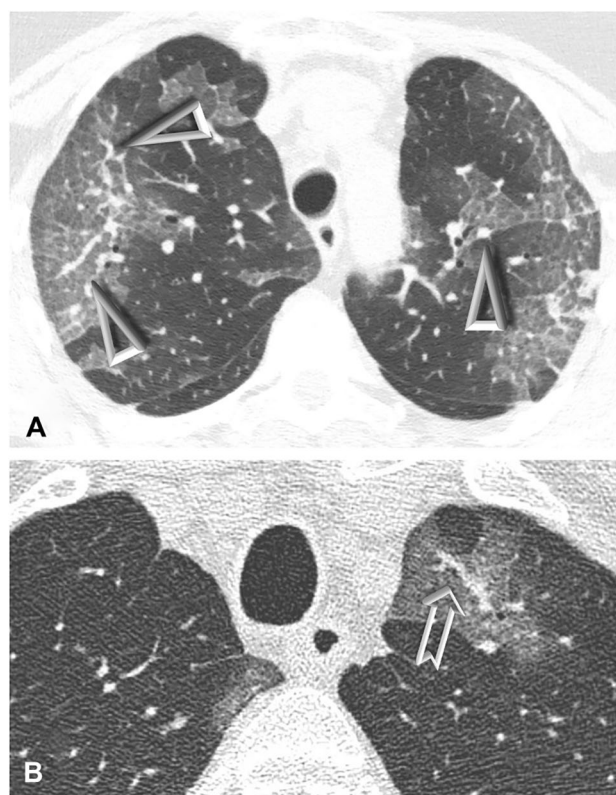

Fig. 1 CT scans showing vascular enlargement pattern (VEP) and vascular tree-in-bud (TIB) in two patients with COVID-19 pneumonia. Notes: A—Bilateral peripheral areas of ground-glass opacification and crazy paving in the upper lobes. Dilated segmental and subsegmental vessels (VEP—arrowheads) are visible inside these areas. B—Targeted image shows striking dilatation of peripheral subpleural vessel in upper left lobe with a branching aspect resembling a budding tree (arrow). Please note that vascular TIB is visible only within the area of ground-glass-opacity in this picture

11 ± 7.5 VFD [16], and considering an α-error of 0.05 and a β-error of 0.8 with a 1:1 ratio between the two groups, a sample size of at least 126 patients was required.

Data collection

Baseline data and patient's history were collected using an electronic case report form developed by YGHEA, CRO division of Ecol Studio SPA (Bologna Operational Headquarters, Bologna, Italy) and hosted by Actide Nubilaria (Novara, Italy). Collected data included demographic data, underlying comorbidities, laboratory data, chest radiological reports, respiratory parameters before the intubation and during the first five days of IMV (static compliance—C_{RS}, PaO_2/FiO_2 ratio), and clinical outcomes.

Radiological data recorded consisted in the presence, extent and distribution of VEP, TIB and peripheral micronodules, scored on the basis of the number of lobes involved; GGO, crazy paving and consolidations, evaluated

for percentage of lung involvement on a scale of 0 to 4 as follows: 0 = 0% involvement, 1 = less than 25%, 2 = 25% to less than 50%, 3 = 50% to less than 75%, 4 = 75% or greater involvement. The concomitant presence of pleural effusion and pulmonary artery dilatation (diameter greater than 29 mm) were also recorded.

Concerning the extent of the lesions, VEP, TIB and peripheral nodules were considered extended if they involved 3 or more lobes, while GGO, crazy paving and consolidations were considered extended if they involved more than 50% of the pulmonary parenchyma.

Concerning pronation-related data, the PaO_2/FiO_2 was recorded within 3 h before prone positioning (T1) and from 1 to 3 h after re-supination (T2), all data were referred to the first pronation and both measurements were taken, therefore, in the supine position, and the duration of the PP session was recorded. A PaO_2/FiO_2 increase of at least 49% was used as a cut-off value to identify responders to pronation [15].

CT scan acquisition

Chest CT studies were interpreted by the means of a consensus assessment from two radiologists with at least 5 years of experience for each centre. If consensus was not reached, a senior radiologist was consulted to address the final decision.

CT scan acquisitions were performed using different scanners in different institutions: GE VCT Lightspeed 64, GE VCT Lightspeed 16 (GE Healthcare, Buckinghamshire, UK), Philips CT Ingenuity 64, Philips Brilliance 64 (Philips Medical Systems, Best, The Netherlands), Toshiba Aquilion S16 TSX-101A and Toshiba Aquilion S32 TSX-101A (Toshiba Medical Systems Europe, Zoetermeer, The Netherlands).

The scans included non-contrast acquisition and were obtained in the supine position from lung apices to bases at full-suspended inspiration, with ≤ 1.25-mm section thicknesses, using standard acquisition parameters adjusted to patients' biometrics (100–120 effective mAs and 120–140 kVp). Images were reconstructed using both sharp kernels and visualized at window settings optimized for lung parenchyma (window width, 1500 HU; window level, -500 HU), and medium-soft kernels with soft-tissue window settings (window width, 300 HU; window level, 40 HU). Maximum intensity projection (MIP) images were used to facilitate the recognition of the TIB and VEP.

Statistical analysis

Data were analysed using Stata/CI 16 (StataCorp LLC, Texas, USA) and GraphPad Prism version 8.4.3 for Windows (GraphPad Software, San Diego, California, USA).

Continuous variables were tested for normality with the Shapiro–Wilk test and were expressed as mean and standard deviation (SD) or median and interquartile range [IQR] based on their distribution. Comparisons between continuous variables were made with the Student's t-test or the Mann–Whitney U test when appropriate. Categorical variables were expressed as numbers and percentages and compared using the Chi-square test or Fisher's exact test when needed.

The log-rank test was used to compare the cumulative incidences of liberation from mechanical ventilation up to day 28 between the groups of patients with and without TIB and VEP. Kaplan–Meier curves were also built for the same groups.

Finally, bivariate Spearman correlation coefficients were calculated taking into account the extension of the different radiological signs.

Results

During the study period, 632 patients were assessed for eligibility. After excluding those who underwent exclusively NIV or with missing data, the original study enrolled a total of 470 patients. Of these, 139 had a CT scan performed within ± 3 days from orotracheal intubation and were therefore included in the final analysis; supplement Fig. 1 shows the flow of the patients throughout the study.

Globally, the TIB sign was observed in 75 out of the 139 patients (54%), while the VEP in 108 out of 139 (77.7%); Table 1 shows the main demographic and clinical variables of the patients included, while Table 2 describes their clinical course.

The TIB sign was associated with a significantly lower BMI and a small, but statistically significant, delay from hospital to ICU admission and orotracheal intubation; these differences were not observed concerning the presence of the VEP. Patients' demographics were not significantly different with regard to age, comorbidities, clinical severity at ICU admission (SAPS II and SOFA score) as well as for the clinical severity of COVID-19-related ARDS in terms of worst PaO_2/FiO_2 ratio and lowest respiratory system compliance (C_{RS}) observed during the first five days of IMV for both the TIB and VEP comparisons.

Supplement Table 1 shows the initial laboratory and ventilatory data. The nearest D-dimer concentration from the CT scan as well as the peak concentration of IL-6 and LDH was not significantly different between the two groups; however, the prevalence of patients with LDH > 250 U/L [22] was significantly higher in the VEP group (99% vs 85.7%, $p = 0.008$). There were no significant differences in terms of responders to prone positioning either in the TIB (58.7% vs 55.8%, $p = 0.832$) and VEP groups (50.8% vs 73.1%, $p = 0.063$).

Table 1 Demographics, comorbidities, orotracheal intubation timing and ICU admission severity

	All (n = 139)	TIB (n = 75)	No TIB (n = 64)	p	VEP (n = 108)	No VEP (n = 31)	p
Demographics and comorbidities							
Age—yr (IQR)	66 (57–74)	67 (59–74)	64 (57–74)	0.404	68 (59–74)	63 (56–70)	0.115
Sex—male—no (%)	104 (74.8%)	54 (72%)	50 (78.1%)	0.407	80 (74.1%)	24 (77.4%)	0.705
BMI—median (IQR)	28 (25–32)	28 (25–31)	29 (26–33)	**0.033**	28 (25–31)	28 (25–33)	0.838
Hypertension—no (%)	86 (61.9%)	41 (54.7%)	45 (70.3%)	0.058	65 (60.2%)	21 (67.7%)	0.445
Chronic ischemic heart disease—no (%)	12 (8.6%)	5 (6.7%)	7 (10.9%)	0.372	8 (7.4%)	4 (12.9%)	
Chronic kidney disease (CKD)				0.567*			0.790*
CKD—not in dialysis—no (%)	7 (5.0%)	2 (3.1%)	5 (6.7%)		6 (5.6%)	1 (3.2%)	
CKD—patients in dialysis—no (%)	3 (2.2%)	2 (2.7%)	1 (1.6%)		2 (1.9%)	1 (3.2%)	
COPD—no (%)	8 (5.8%)	6 (8.0%)	2 (3.1%)	0.267*	6 (5.6%)	2 (6.5%)	0.852*
COPD—home oxygen therapy/CPAP—no (%)	1 (0.7%)	0 (0%)	1 (1.6%)		1 (0.9%)	0 (0%)	
Diabetes—no (%)	36 (25.9%)	18 (24%)	18 (28.1%)	0.580	30 (27.8%)	6 (19.4%)	0.345
ICU admission and orotracheal intubation							
Time from hospital admission to ICU admission—d (IQR)	1 (0–2)	1 (1–3)	1 (0–2)	**0.004**	1 (0–3)	1 (0–2)	0.089
Time from hospital admission to intubation—d (IQR)	1 (0–3)	2 (1–3)	1 (0–2)	**0.002**	1 (0–3)	1 (0–2)	0.108
SAPS II score	35 (29–43)	35 (29–43)	35 (30–46)	0.488	35 (29–43)	35 (29–46)	0.757
SOFA score at ICU admission	5 (3–7)	5 (3–7)	5 (3–7)	0.790	5 (3–7)	5 (3–7)	0.927

BMI body mass index, *CKD* chronic kidney disease, *COPD* chronic obstructive pulmonary disease, *ICU* intensive care unit, *SAPS* simplified acute physiology score, *SOFA* sequential organ failure assessment, *IQR* interquartile range

Significant *p* values are reported in bold. *Refers to the p value of the Chi-square test for the whole contingency table for the variable taken into account

Table 3 shows the extent and distribution of the main radiologic signs found in the CT scans included, while Fig. 2 represents the correlation matrix of the radiologic variables taken into account. In most cases, both TIB and VEP involved two or three lobes; the extents of the two signs were significantly intercorrelated and also correlated with the percentage of pulmonary parenchyma affected by GGO. The magnitude of the association was weak to moderate (rho coefficients range: 0.32–0.35, *p* < 0.01), TIB extent was also significantly correlated with the extent of peripheral micronodules (rho: 0.26, *p* < 0.01).

Vascular TIB was mostly observed within the GGO areas, while VEP was observed inside the GGO areas in 61.1% and both inside and outside the GGO areas in 34.3% of the cases.

Interestingly, pulmonary artery enlargement was significantly more frequently observed in patients with TIB sign, while this observation was not confirmed for VEP.

Duration of mechanical ventilation was similar between patients with and without TIB in CT scan (15 [8–23] versus 16 [8–24], respectively, *p* = 0.297) as well as 28d-VFD (0 [0–15] vs 0 [0–12], *p* = 0.979). Similar results were found when dividing the two groups based on the presence of the VEP. Figure 3 shows the Kaplan–Meier graph for the cumulative incidence of liberation from mechanical ventilation within the first 28 days after orotracheal intubation based on the presence of the TIB sign or the VEP and the relative log-rank tests; no differences were found in the two functions.

Finally, ICU cardiovascular complications and the need for renal replacement therapy were not significantly different in either of the two grouping modalities (VEP and TIB presence), as well as ICU mortality (Table 2).

Figure 4 shows the distribution of extended radiological signs among different subgroups of patients.

Extended VEP and TIB signs were significantly more frequent in poor responders to pronation, while consolidations were more frequent in responders. Ground glass and crazy paving pattern extension over 50% of pulmonary parenchyma were significantly more frequent in non-survivors. No differences were observed among the radiologic signs concerning weaning from MV within day 28 and PaO$_2$/FiO$_2$ ratio before orotracheal intubation.

Discussion

Microvascular involvement is a key determinant of COVID-19 syndrome, and microvascular signs such as VEP and TIB are part of the typical radiological aspects of this syndrome and have an established role in its diagnosis [8, 12, 23].

Table 2 Ventilatory data, adjunctive therapies, ICU stay and outcomes

	All (n=139)	TIB (n=75)	No TIB (n=64)	p	VEP (n=108)	No VEP (n=31)	p
Mechanical ventilation—first 5 days and adjunctive therapies							
Lowest PaO_2/FiO_2 ratio in supine position—(IQR)	99 (72–132)	102 (70–133)	90 (75–129)	0.546	100 (72–133)	90 (65–115)	0.360
Lowest PaO_2/FiO_2 ratio in supine position—no (%)				0.098*			0.434*
200–300—no (%)	6 (4.3%)	4 (5.3%)	2 (3.1%)		5 (4.6%)	1 (3.2%)	
100–200—no (%)	62 (44.6%)	39 (52.0%)	23 (35.9%)		51 (47.2%)	11 (35.5%)	
<100—no (%)	71 (51.1%)	32 (42.7%)	39 (60.9%)		52 (48.1%)	19 (61.3%)	
Lowest static C_{RS}—mL/cmH2O (IQR)	40 (32–47)	39 (30–47)	40 (35–48)	0.186	40 (32–47)	40 (30–48)	0.950
C_{RS} <40 mL/cmH2O—no (%)	65 (46.8%)	38 (50.7%)	27 (42.2%)	0.318	49 (45.4%)	16 (51.6%)	0.539
Neuromuscular blocking agents continuous infusion—no (%)	124 (89.1%)	67 (89.3%)	57 (89.1%)	0.959	97 (89.8%)	27 (87.1%)	0.667
Any thromboprophylaxis—no (%)	139 (100%)	75 (100%)	64 (100%)	1.000	108 (100%)	31 (100%)	1.000
Enoxaparin therapy—no (%)	184 (89.2%)	69 (92%)	55 (85.9%)	0.251	97 (89.8%)	27 (87.1%)	0.667
Enoxaparin daily dose—mg (IQR)	60 (40–80)	60 (40–80)	60 (40–80)	0.393	60 (40–80)	60 (40–80)	0.782
Intravenous corticosteroids—no (%)	96 (69.1%)	56 (74.7%)	40 (62.5%)	0.122	77 (71.3%)	19 (61.3%)	0.288
Antiplatelet therapy—no (%)	44 (31.7%)	24 (32%)	20 (31.3%)	0.925	33 (30.6%)	11 (35.5%)	0.603
ICU stay and outcomes							
Tracheotomy—no (%)	89 (64.0%)	44 (58.7%)	45 (70.3%)	0.154	72 (66.7%)	17 (54.8%)	0.226
Prone positioning—no (%)	83 (59.7%)	43 (57.3%)	40 (62.5%)	0.536	65 (60.2%)	18 (58.1%)	0.832
Cardiovascular complications—no (%)	35 (25.2%)	21 (28.0%)	14 (21.9%)	0.407	28 (25.9%)	7 (22.6%)	0.705
Need for RRT—no (%)	31 (22.3%)	14 (18.7%)	17 (26.6%)	0.265	26 (24.1%)	5 (16.1%)	0.349
Duration of MV—days (IQR)	15 (9–24)	15 (8–23)	16 (8–24)	0.297	15 (9–24)	16 (9–23)	0.652
VFD-28 days—days (IQR)	0 (0–14)	0 (0–15)	0 (0–12)	0.979	0 (0–15)	0 (0–12)	0.980
ICU length of stay—days (IQR)	18 (12–32)	19 (13–31)	17 (9–33)	0.558	19 (13–32)	17 (9–33)	0.652
ICU mortality—no (%)	57 (41.0%)	32 (42.7%)	25 (39.1%)	0.667	46 (42.6%)	11 (35.5%)	0.478

C_{RS} respiratory system compliance, *IQR* interquartile range

Significant *p* values are reported in bold. *Refers to the *p* value of the Chi-square test for the whole contingency table for the variable taken into account

However, the clinical implications of these signs are still poorly investigated.

The main findings of this study were: (a) the evidence of VEP or TIB on CT scans performed within 3 days from oro-tracheal intubation was not associated with different clinical courses in terms of duration of MV or mortality; (b) no differences were either found about the median concentration of biomarkers related to disease severity and thrombosis; however, VEP was significantly associated with a slightly higher prevalence of LDH > 250 U/L and TIB was associated with an increased prevalence of pulmonary artery enlargement; (c) the extent of microvascular signs was significantly correlated with that of GGO, peripheral micronodules and crazy paving pattern, while no correlation was found with the extent of consolidations; (d) the involvement of 3 or more lobes by VEP and TIB was more frequent among non-responders to prone positioning.

Recent literature found a significant association between the evidence of VEP or TIB in CT scan imaging and disease severity in terms of symptoms and biomarkers, impaired coagulation and an increase in the duration of MV and hospital stay [7, 23].

Among COVID-19 patients showing vascular changes in CT scan, a significantly increased proportion of elevated C-reactive protein and LDH was observed [23], and the elevation of these biomarkers was significantly associated with ICU admission and mortality in the available literature [1, 24].

Our results showed no differences in median values of LDH; however, VEP was associated with a significantly increased proportion of patients with peak LDH values above 250 U/L during the first 7 days of hospitalization [22].

On the other hand, TIB was associated with a significantly increased prevalence of pulmonary artery dilatation, a radiologic sign recently recognized as a predictor of clinical severity and mortality in COVID-19 patients [25, 26].

However, despite the higher prevalence of negative prognostic factors in the VEP and TIB populations, we were not able to demonstrate any significant difference in terms of liberation from mechanical ventilation and mortality.

Table 3 Main radiologic findings

Vascular signs and peripheral nodules—number of lobes involved

	Present	1	2	3	4	5
Vascular tree in bud—no (%)	75 (54%)	7 (9.3%)	26 (34.7%)	23 (30.7%)	9 (12%)	10 (13.3%)
Vascular enlargement pattern—no (%)	108 (77.7%)	3 (2.8%)	24 (22.2%)	26 (24.1%)	17 (15.7%)	38 (35.2%)
Peripheral nodules—no (%)	24 (17.3%)	2 (8.3%)	10 (41.7%)	9 (37.5%)	3 (12.5%)	0 (0%)

Vascular signs and peripheral nodules—distribution and localization

	Distribution			Localization		
	Anterior	Intermediate	Posterior	Inside GGO	Outside GGO	Both
Vascular tree in bud ($n=75$)—no (%)	43 (57.3%)	59 (78.7%)	38 (50.7%)	63 (84%)	0 (0%)	12 (16%)
Vascular enlargement pattern ($n=108$)—no (%)	74 (68.5%)	89 (82.4%)	80 (74.1%)	66 (61.1%)	5 (4.6%)	37 (34.3%)
Peripheral nodules ($n=24$)—no (%)	12 (50%)	20 (83.3%)	9 (37.5%)	16 (66.7%)	2 (8.3%)	6 (25.0%)

Ground glass opacities, crazy paving and consolidations—visual extension and distribution

	Present	1–25%	26–50%	51–75%	76–100%	Main distribution (A/P/D)
Ground glass opacities—no (%)	131 (94.2%)	49 (37.4%)	35 (26.7%)	31 (23.7%)	16 (12.2%)	A - 21 (16%) P - 4 (3.1%) D - 106 (80.9%)
Crazy paving—no (%)	71 (51.1%)	37 (52.1%)	15 (21.1%)	15 (21.1%)	4 (5.6%)	A - 14 (19.7%) P - 9 (12.7%) D - 48 (67.6%)
Consolidations—no (%)	120 (86.3%)	76 (63.3%)	35 (29.2%)	5 (4.2%)	4 (3.3%)	A - 5 (4.2%) P - 89 (74.2%) D - 26 (21.7%)

Other radiologic findings

	TIB ($n=75$)	No TIB ($n=64$)	p	VEP ($n=108$)	No VEP ($n=31$)	p
Pleural effusion—n (%)			0.467[*]			0.260[*]
Monolateral	6 (8%)	2 (3.1%)		5 (4.6%)	3 (9.7%)	
Bilateral	7 (9.3%)	6 (9.4%)		12 (11.1%)	1 (3.2%)	
Pulmonary artery enlargement (> 29 mm)—n (%)	52 (69.3%)	23 (35.9%)	**< 0.001**	60 (55.6%)	15 (48.4%)	0.480

Main distribution: *A* anterior, *P* posterior, *D* diffuse

Significant *p* values are reported in bold. *Refers to the *p* value of the Chi-square test for the whole contingency table for the variable taken into account

Moreover, the number of lobes involved by VEP and TIB was correlated with a higher extent of the GGO (Fig. 2), which has been already associated with worse outcomes in several studies [27–29], and this aspect was also confirmed in our study where we found a significantly higher prevalence of extended GGO among non-survivors (Fig. 4).

The pulmonary epithelial and endothelial damage due to SARS-CoV-2, the subsequent release of inflammatory cytokines and the proinflammatory/anti-inflammatory unbalance seem to be a shared mechanism between the development of the microvascular abnormalities, oedema and exudate formation [30], of which GGOs are the radiologic expression [23, 31].

Therefore, based on our results, VEP and TIB extent could be a partial epiphenomenon of GGO extent, without a prognostic significance in terms of duration of IMV or mortality in critically ill patients.

Interestingly, extended microvascular signs were significantly more frequent among non-responders to prone positioning, this aspect is in line with our previous research [15], which found that the PaO_2/FiO_2 increase observed after prone positioning in sustained responders could not be fully explained by differences in driving pressure. Possibly, disease phenotypes showing an extensive microvascular involvement could blunt the oxygenation response to prone positioning, while phenotypes showing extended
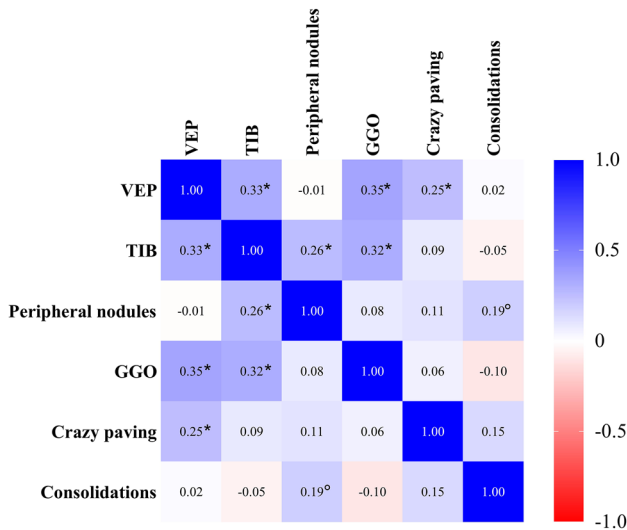
Fig. 2 Spearman heatmap regarding the extension of the radiologic signs explored. Abbreviations: VEP—vascular enlargement pattern; TIB—tree in bud sign; GGO—ground glass opacities. Notes—the values reported in the cells refer to the rho coefficient for the bivariate correlation of the two variables; $p < 0.05$; *$p < 0.01$

consolidations rely more on parenchymal recruitment and ventilation/perfusion ratio redistribution for their oxygenation response.

Unfortunately, prone positioning was performed in only 83 (59.7%) of the patients enrolled in the present study; therefore, we were limited in performing subgroup analyses concerning the anteroposterior distribution of vascular lesions or extent of consolidations. The mixed population of patients treated and not treated with prone positioning in this study could have also played a role concerning the observed liberation from MV.

Our results could have also been partially influenced by the selection criteria adopted for patients' enrolment because, since this study focused exclusively on critically ill COVID-19 patients, a higher prevalence of negative prognostic risk factors is expected, and the relative eventual prognostic value of vascular signs could have been smoothened in favour of other factors that notoriously play a role in critically ill patients such as the number of concomitant organ failures [16, 32], hospital-acquired superinfections [33, 34] and other ICU complications [2, 35].

Another limitation of this study is related to the different experimental treatments that were adopted for patients undergoing IMV during the study period and that could have partially influenced our results.

Moreover, we could not get more detailed lung perfusion images due to the lack of systematic acquisition of pulmonary CT angiograms in the patients included and the unavailability of dual-energy computed tomography (DECT) machines in the centres participating in this study, differently from previous works [7]. Finally, it should be noted that consolidations imply the increase in parenchymal attenuation that obscures the margins of vessels, and this may have influenced the prevalence of microvascular signs in patients demonstrating more consolidated lung areas.

Future research should further define if vascular signs are only a radiologic epiphenomenon of a common shared pathogenetic mechanism with GGO or have an independent clinical meaning and their eventual relation with COVID-19-related coagulopathy.
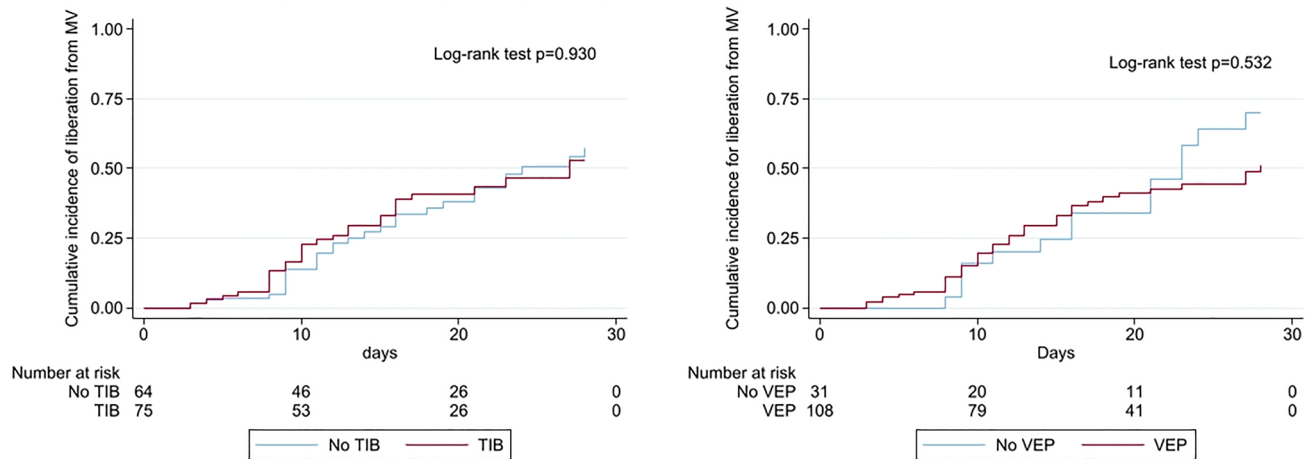
Fig. 3 Cumulative incidence functions of liberation from mechanical ventilation. Abbreviations: TIB—tree in bud; VEP—vascular enlargement pattern; MV—mechanical ventilation
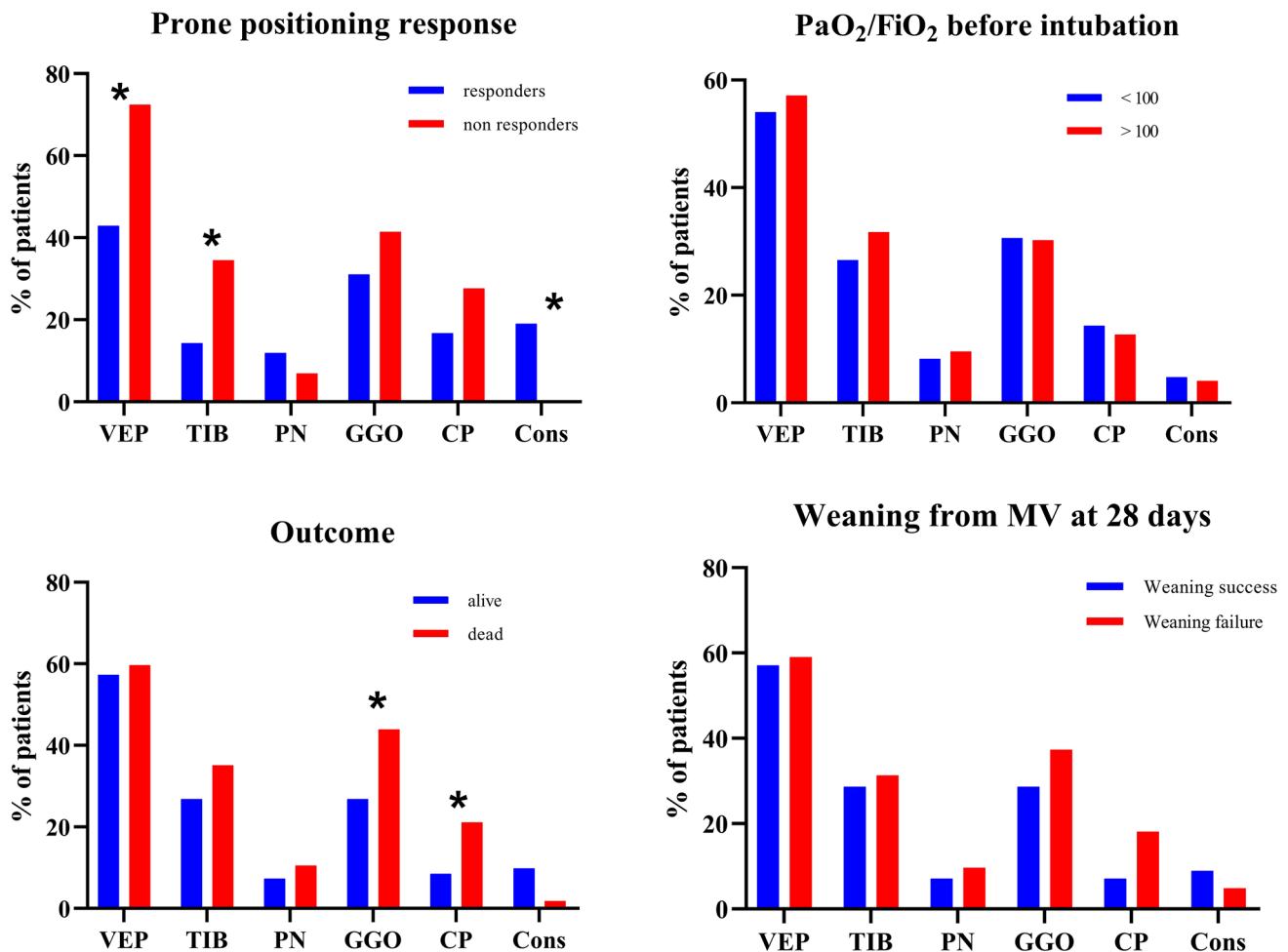
Fig. 4 Prevalence of extended radiologic signs in different contexts. Abbreviations: VEP—vascular enlargement pattern; TIB—tree in bud; PN—peripheral nodules; GGO—ground glass opacities; CP—crazy paving; Cons—consolidations. Notes: Graphs show the prevalence of VEP, TIB and PN involving 3 or more lobes and GGO, CP and Cons extended for over the 50% of pulmonary parenchyma. $*p < 0.05$ at Chi-square test

Conclusions

Vascular TIB and VEP are frequently observed in the CT scans of critically ill COVID-19 patients requiring IMV. Their extent is significantly correlated with GGO and crazy paving pattern areas. Despite previous studies suggesting a potential prognostic role of these signs concerning the duration of IMV and survival, and the detection of a higher prevalence of prognostic factors associated with prolonged ventilation in our population, we were not able to confirm this hypothesis.

Patients not responding to prone positioning had a higher extent of microvascular involvement signs. More focused studies on the potential relation between vascular signs and oxygenation response to prone positioning could better clarify if these signs could help in choosing which patients may benefit from prone positioning.

Declarations

References

1. Wu Z, McGoogan JM (2020) Characteristics of and important lessons from the coronavirus disease 2019 (COVID-19) outbreak in China: summary of a report of 72314 cases from the chinese center for disease control and prevention. JAMA J Am Med Assoc 323:1239–1242

2. Lodigiani C, Iapichino G, Carenzo L et al (2020) Venous and arterial thromboembolic complications in COVID-19 patients admitted to an academic hospital in Milan, Italy. Thromb Res 191:9–14. https://doi.org/10.1016/j.thromres.2020.04.024

3. Helms J, Tacquard C, Severac F et al (2020) High risk of thrombosis in patients with severe SARS-CoV-2 infection: a multicenter prospective cohort study. Intensive Care Med 46:1089–1098. https://doi.org/10.1007/s00134-020-06062-x

4. Ackermann M, Verleden SE, Kuehnel M et al (2020) Pulmonary vascular endothelialitis, thrombosis, and angiogenesis in Covid-19. N Engl J Med 383:120–128. https://doi.org/10.1056/nejmoa2015432

5. Loo J, Spittle DA, Newnham M (2021) COVID-19, immunothrombosis and venous thromboembolism: biological mechanisms. Thorax 76:412–420. https://doi.org/10.1136/thoraxjnl-2020-216243

6. Grasselli G, Tonetti T, Protti A et al (2020) Pathophysiology of COVID-19-associated acute respiratory distress syndrome: a multicentre prospective observational study. Lancet Respir Med 8:1201–1208. https://doi.org/10.1016/S2213-2600(20)30370-2

7. Patel BV, Arachchillage DJ, Ridge CA et al (2020) Pulmonary angiopathy in severe COVID-19: physiologic, imaging, and hematologic observations. Am J Respir Crit Care Med 202:690–699. https://doi.org/10.1164/rccm.202004-1412OC

8. Li Q, Huang XT, Li CH et al (2021) CT features of coronavirus disease 2019 (COVID-19) with an emphasis on the vascular enlargement pattern. Eur J Radiol. https://doi.org/10.1016/j.ejrad.2020.109442

9. Lv H, Chen T, Pan Y et al (2020) Pulmonary vascular enlargement on thoracic CT for diagnosis and differential diagnosis of COVID-19: a systematic review and meta-analysis. Ann Transl Med 8:878–878. https://doi.org/10.21037/atm-20-4955

10. Bai HX, Hsieh B, Xiong Z et al (2020) Performance of radiologists in differentiating COVID-19 from non-COVID-19 viral pneumonia at chest CT. Radiology 296:E46–E54. https://doi.org/10.1148/radiol.2020200823

11. Caruso D, Zerunian M, Polici M et al (2020) Chest CT features of COVID-19 in Rome, Italy. Radiology 296:E79–E85. https://doi.org/10.1148/radiol.2020201237

12. Zhou S, Wang Y, Zhu T, Xia L (2020) CT features of coronavirus disease 2019 (COVID-19) pneumonia in 62 patients in Wuhan, China. Am J Roentgenol 214:1287–1294. https://doi.org/10.2214/AJR.20.22975

13. Liu J, Zheng X, Tong Q et al (2020) Overlapping and discrete aspects of the pathology and pathogenesis of the emerging human pathogenic coronaviruses SARS-CoV, MERS-CoV, and 2019-nCoV. J Med Virol 92:491–494. https://doi.org/10.1002/jmv.25709

14. Eddy RL, Sin DD (2020) Computed tomography vascular tree-in-bud: a novel prognostic imaging biomarker in COVID-19? Am J Respir Crit Care Med 202:642–644. https://doi.org/10.1164/rccm.202007-2833ED

15. Scaramuzzo G, Gamberini L, Tonetti T et al (2021) Sustained oxygenation improvement after first prone positioning is associated with liberation from mechanical ventilation and mortality in critically ill COVID-19 patients: a cohort study. Ann Intensive Care 11:1–10. https://doi.org/10.1186/s13613-021-00853-1

16. Gamberini L, Tonetti T, Spadaro S, et al (2020) Factors influencing liberation from mechanical ventilation in coronavirus disease 2019: multicenter observational study in fifteen Italian ICUs. 4:1–12

17. Tack D, Nollevaux MC, Gevenois PA (2001) Tree-in-bud pattern in neoplastic pulmonary emboli. Am J Roentgenol 176:1421–1422. https://doi.org/10.2214/ajr.176.6.1761421

18. Lang M, Som A, Carey D et al (2020) Pulmonary vascular manifestations of COVID-19 pneumonia. Radiol Cardiothorac Imaging 2:e200277. https://doi.org/10.1148/ryct.2020200277

19. Hansell DM, Bankier AA, Mcloud TC et al (2008) Fleischner society: glossary of terms for thoracic imaging. Radiology 246:697

20. Yehya N, Harhay MO, Curley MAQ et al (2019) Reappraisal of ventilator-free days in critical care research. Am J Respir Crit Care Med 200:828–836. https://doi.org/10.1164/rccm.201810-2050CP

21. Ranieri VM, Rubenfeld GD, Thompson BT et al (2012) Acute respiratory distress syndrome: the Berlin definition. JAMA J Am Med Assoc 307:2526–2533. https://doi.org/10.1001/jama.2012.5669

22. Huang H, Cai S, Li Y et al (2020) Prognostic factors for COVID-19 pneumonia progression to severe symptoms based on earlier clinical features: a retrospective analysis. Front Med 7:1–7. https://doi.org/10.3389/fmed.2020.557453

23. Şanli DET, Yildirim D (2021) A new imaging sign in COVID-19 pneumonia: vascular changes and their correlation with clinical severity of the disease. Diagn Interv Radiol 27:172–180. https://doi.org/10.5152/dir.2020.20346

24. Herold T, Jurinovic V, Arnreich C et al (2020) Elevated levels of IL-6 and CRP predict the need for mechanical ventilation in COVID-19. J Allergy Clin Immunol 146:128-136.e4. https://doi.org/10.1016/j.jaci.2020.05.008

25. Esposito A, Palmisano A, Toselli M et al (2021) Chest CT-derived pulmonary artery enlargement at the admission predicts overall survival in COVID-19 patients: insight from 1461 consecutive patients in Italy. Eur Radiol 31:4031–4041. https://doi.org/10.1007/s00330-020-07622-x

26. Zhu QQ, Gong T, Huang GQ et al (2021) Pulmonary artery trunk enlargement on admission as a predictor of mortality in in-hospital patients with COVID-19. Jpn J Radiol 39:589–597. https://doi.org/10.1007/s11604-021-01094-9

27. Malpani Dhoot N, Goenka U, Ghosh S et al (2020) Assigning computed tomography involvement score in COVID-19 patients: prognosis prediction and impact on management. BJR Open 2:20200024. https://doi.org/10.1259/bjro.20200024

28. Carvalho ARS, Guimarães A, Werberich GM et al (2020) COVID-19 chest computed tomography to stratify severity and disease extension by artificial neural network computer-aided diagnosis. Front Med 7:1–11. https://doi.org/10.3389/fmed.2020.577609

29. Ruch Y, Kaeuffer C, Ohana M et al (2020) CT lung lesions as predictors of early death or ICU admission in COVID-19 patients. Clin Microbiol Infect 26:1417.e5-1417.e8. https://doi.org/10.1016/j.cmi.2020.07.030

30. Levi M, Coppens M (2021) Vascular mechanisms and manifestations of COVID-19. Lancet Respir Med 9:551–553. https://doi.org/10.1016/s2213-2600(21)00221-6

31. Mokhtari T, Hassani F, Ghaffari N et al (2020) COVID-19 and multiorgan failure: a narrative review on potential mechanisms. J Mol Histol 51:613–628. https://doi.org/10.1007/s10735-020-09915-3

32. Stephens JR, Stümpfle R, Patel P et al (2020) Analysis of critical care severity of illness scoring systems in patients with coronavirus disease 2019: a retrospective analysis of three UK ICUs. Crit Care Med 49:E105–E107

33. Bardi T, Pintado V, Gomez-Rojo M et al (2021) Nosocomial infections associated to COVID-19 in the intensive care unit: clinical characteristics and outcome. Eur J Clin Microbiol Infect Dis 40:495–502. https://doi.org/10.1007/s10096-020-04142-w

34. Ippolito M, Misseri G, Catalisano G et al (2021) Ventilator-associated pneumonia in patients with covid-19: a systematic review and meta-analysis. Antibiotics 10:1–19. https://doi.org/10.3390/antibiotics10050545

35. Potere N, Valeriani E, Candeloro M et al (2020) Acute complications and mortality in hospitalized patients with coronavirus disease 2019: a systematic review and meta-analysis. Crit Care 24:1–12. https://doi.org/10.1186/s13054-020-03022-1

Authors and Affiliations

Giorgia Dalpiaz[1] · Lorenzo Gamberini[2] · Aldo Carnevale[3] · Savino Spadaro[4] · Carlo Alberto Mazzoli[2] · Sara Piciucchi[5] · Davide Allegri[6] · Chiara Capozzi[7] · Ersenad Neziri[8] · Maurizio Bartolucci[9] · Francesco Muratore[10] · Francesca Coppola[11] · Antonio Poerio[12] · Emanuela Giampalma[13] · Luca Baldini[14] · Tommaso Tonetti[15] · Iacopo Cappellini[16] · Davide Colombo[17,18] · Gianluca Zani[19] · Lorenzo Mellini[20] · Vanni Agnoletti[21] · Federica Damiani[22] · Giovanni Gordini[2] · Cristiana Laici[23] · Giuliano Gola[24] · Antonella Potalivo[25] · Jonathan Montomoli[26] · Vito Marco Ranieri[15] · Emanuele Russo[21] · Stefania Taddei[27] · Carlo Alberto Volta[4] · Gaetano Scaramuzzo[4]

1   Department of Radiology, Bellaria Hospital, Bologna, Italy

2   Department of Anaesthesia, Intensive Care and Prehospital Emergency, Ospedale Maggiore Carlo Alberto Pizzardi, Bologna, Italy

3   Department of Radiology, Azienda Ospedaliero-Universitaria S. Anna, Via Aldo Moro, 8, 44121 Cona, Ferrara, Italy

4   Department of Morphology, Surgery and Experimental Medicine, Section of Anaesthesia and Intensive Care, University of Ferrara, Azienda Ospedaliero-Universitaria S. Anna, Via Aldo Moro, 8, 44121 Cona, Ferrara, Italy

5   Department of Radiology, G. B. Morgagni Hospital, Forlì, Italy

6   Department of Clinical Governance and Quality, Bologna Local Healthcare Authority, Bologna, Italy

7   IRCCS Azienda Ospedaliero-Universitaria Di Bologna, Bologna, Italy

8   Radiology Department, SS. Trinità Hospital, ASL Novara, Borgomanero, Italy

9   Radiology Department, Azienda USL Toscana Centro, Prato, Italy

10   Radiology Department, Infermi Hospital, Rimini, Italy

11   Department of Radiology, IRCCS Azienda Ospedaliero-Universitaria di Bologna, Via Albertoni 15, 40138 Bologna, Italy

12   Department of Radiology, Imola Hospital, Imola, Italy

13   Radiology Department, M. Bufalini Hospital, Cesena, Italy

14   Department of Radiology, University Hospital of Modena, Via del Pozzo 71, 41100 Modena, Italy

[15] Alma Mater Studiorum, Dipartimento di Scienze Mediche e Chirurgiche, Anesthesia and Intensive Care Medicine, Policlinico di Sant'Orsola, Università di Bologna, Bologna, Italy

[16] Department of Critical Care Section of Anesthesiology and Intensive Care, Azienda USL Toscana Centro, Prato, Italy

[17] Traslational Medicine Department, Eastern Piedmont University, Novara, Italy

[18] Anesthesiology Department, SS. Trinità Hospital, ASL Novara, Borgomanero, Italy

[19] Department of Anesthesia and Intensive Care, Santa Maria Delle Croci Hospital, Ravenna, Italy

[20] Department of Radiology, Santa Maria Delle Croci Hospital, Ravenna, Italy

[21] Anaesthesia and Intensive Care Unit, M. Bufalini Hospital, Cesena, Italy

[22] Department of Anaesthesia, Intensive Care and Pain Therapy, Imola Hospital, Imola, Italy

[23] Division of Anesthesiology, Hospital S. Orsola Malpighi, Alma Mater Studiorum University of Bologna, Bologna, Italy

[24] Department of Radiology, Azienda Ospedaliera SS. Antonio e Biagio e Cesare Arrigo, Alessandria, Italy

[25] Department of Anaesthesia and Intensive Care, Ospedale degli Infermi, Faenza, Italy

[26] Department of Anaesthesia and Intensive Care, Infermi Hospital, Rimini, Italy

[27] Anaesthesia and Intensive Care Unit, Bentivoglio Hospital, Bentivoglio, Italy